Journal of Molecular Liquids 394 (2024) 123725

Contents lists available at ScienceDirect

Journal of Molecular Liquids

journal homepage: www.elsevier.com/locate/molliq

Preparation of ionic liquids amine hybrid solvents, characterization for CO_2 absorption, and kinetic performance

Saleem Nawaz Khan [a], Faheem Abbas [b], Francis M. Enujekwu [c], Sami Ullah [d,*], Mohammed Ali Assiri [d], Abdullah G. Al-Sehemi [d]

[a] National University of Science and Technology (NUST), H-12, Islamabad, Pakistan
[b] Key Lab of Organic Optoelectronics and Molecular Engineering of Ministry of Education, Department of Chemistry, Tsinghua University, Beijing 100084, China
[c] Department of Chemical and Environmental Engineering, The University of Nottingham Ningbo China, Ningbo 315100, China
[d] Department of Chemistry, College of Science, King Khalid University, Abha 61413, Saudi Arabia

ARTICLE INFO

Keywords:
Ionic liquids
Methyldiethanolamine
CO_2 capture
Absorption rate
Kinetics study

ABSTRACT

The thermo-physical characteristics of an ionic liquid-amine hybrid solvent were studied in this work as a result of its potential use in the CO_2 absorption process. The hybrid solvents were developed by mixing 30 wt% MDEA with ionic liquid at different concentrations of 5 wt%, 10 wt%, 15 wt% and 20 wt%. Three imidazolium-based ILs were investigated: 1-butyl-3-methylimidazolium dicyanamide [bmim][DCA], 1-butyl-3-methylimidazolium acetate [bmim][Ac] and 1-butyl-3-methylimidazolium trifluoromethanesulfonate [bmim][TfO. Aqueous ionic liquid-amine hybrid solvent's density, surface tension, refractive index, viscosity and were studied between 25 °C and 70 °C with a regular interval of 5 °C. Whereas the influence of temperature on viscosity is negligible beyond 65 °C and the influence of temperature changed certain physicochemical properties. Furthermore, high-pressure solubility tests were conducted at a fixed temperature of 30 °C to determine the solubility of CO_2 in hybrid media at pressures ranging from 2 bar to 50 bar. The results showed that the CO_2 solubility of the different ionic liquid-amine hybrid systems decreases in the following sequence: [bmim][TfO] + MDEA > [bmim][DCA] + MDEA > [bmim][Ac] + MDEA. It was also found out that the optimum concentration of ionic liquids in the solution is 10 wt%. The kinetics study of the hybrid solvents was studied as a function of concentration, and experimentally determined that 10 wt% [bmim][TfO] exhibited the fast CO_2 absorption kinetics. The kinetics performance study was further conducted as a function of pressure, and the highest absorption rate was recorded at 50 bar as expected. Overall, the addition of ionic liquids was verified to improve the CO_2 absorption and thus it was reported that ionic liquid-amine hybrid solvent is an auspicious solvent for CO_2 removal in the future.

1. Introduction

Industrialization, globalization, and population increase are the key factors for continuous increase of energy use throughout the globe. In 2040, alternative sources and nuclear power will make up the majority of new energy capacity, while 78 % of global energy consumption will still come from fossil fuels [1–3]. Natural gas has the highest annual growth rate across fossil resources, with a worldwide utilization rise of 1.9 %. Since carbon dioxide (CO_2) emissions is mainly due to fossil fuel combustion, therefore the discussion about climate change revolves mostly around the topic of energy use. In 2012, the world's energy sector was responsible for 32.3 billion metric tons of the release of carbon dioxide; by 2020, that number is predicted to rise to 35.6 billion metric tons. By 2040, it might reach 43.2 billion metric tons [1,4]. CO_2 is believed to be the primary contributor to the emanation of greenhouse gases (GHGs). Climate change causes serious climate change such as the increase in atmosphere temperature, melting of glaciers and rising in sea levels which risk the well-being of people, the success of farms, the availability of clean water, and the continued existence of natural communities and wildlife. Among fossil fuels, natural gas (NG) is a promising fossil fuel in the future as it has the least carbon-intensive fossil fuel with lower CO_2 emission factor. NG which consists primarily of methane and considerable amounts of light and heavier hydrocarbons, is contaminated with impurities of 2 % CO_2, 4 % N_2 and 4 ppm H_2S. The maximum allowable CO_2 permitted in NG transported to customers need to be less than 3 % [5]. These impurities especially CO_2 can

* Corresponding author.
E-mail addresses: samichemist1@gmail.com, samiali@kku.edu.sa (S. Ullah).

https://doi.org/10.1016/j.molliq.2023.123725
Received 3 June 2023; Received in revised form 16 November 2023; Accepted 1 December 2023
Available online 2 December 2023

be removed from the NG through the purification processes in Acid Gas Removal Unit (AGRU) in order to boost the product's quality [6]. As the dominant GHGs as well as the main NG impurity, CO_2 needs to be captured and separated. The new technology called the Carbon Capture and Storage (CCS) can capture at least ninety percent of carbon dioxide emissions are caused from burning fossil fuels for purposes like power generation and manufacturing [7,8]. The CCS chain consists of capture, transport and storage. Before the CO_2 can be transported for safe storage, capturing carbon dioxide may be done in one of three ways: before combustion, after combustion, or by the use of oxy-fuel [9–12]. As the name implies, post-combustion is when CO_2 is captured from the flue gas after complete combustion with air [13,14]. Afterwards, the exhaled carbon dioxide will be absorbed by the solvent (amines or ammonia) and stored. The flue gas from an industrial power plant enters a scrubbing tank and liquid solvent will then chemically react with and essentially scrubs CO_2 out of the stream, leaving at the bottom of the tank.

CO_2 separation and capturing are carried out using different technologies. CO_2 contained in a gas mixture can be separated through separation techniques such as membrane filtration, cryogenics, chemical and physical adsorption, absorption [14–21]. Among these technologies, absorption is the most industrially established method to separate from bulk gas sources. It is a bulk phenomenon, takes place between a liquid with gas. Typical solvents are amines, potassium carbonate and ammonia-based solutions. Torralba-Calleja et al. [14] described chemical absorption takes place when the CO_2 form covalent bonds with the amines while physical absorption takes place when the CO_2 form van der Waals interaction with ionic liquid, Rectisol, Selexol, and fluorinated solvents [14]. Regeneration of the absorbent is achieved through a heating and/or depressurizing the system to perform a stripping or regenerating procedure [13,14]. In general, absorption technology has high efficiency even though solvent degradation resulting in solvent loss, equipment corrosion and environmental pollution [13,22]. Amines have the best qualities for CO_2 capture because they are highly reactive with CO_2, have a large absorption capacity, are thermally stable at high temperatures, and are very selective for CO_2. Unfortunately, there are some significant drawbacks with this, factors such as elevated corrosion rates of devices and significant energy requirements for regenerating, high volatility, limited CO_2 loading capacity and degradation of amines [23–27]. The high volatility of amine gases into the atmosphere upon heating produces dangerous toxins which causes environmental pollution and harms human health. The corrosive nature of amines, especially MEA corrodes the equipment made of carbon steel, it is reported that MEA operating pilot plants had corrosion rates of 1 mm per year [25]. Compare to the disadvantages of amine in CO_2 capture, ILs are auspicious substitutes with their maximum CO_2 loading of 0.75 mol fraction [28]. ILs are organic compounds made up of ionic species, having melting temperature not more than 373 K [5]. At ambient conditions, ILs maintain a liquid state (room temperature ionic liquids, RTILs). There are several unusual and diverse characteristics properties that make ILs a good alternative solvent to replace conventional amine solvents. It includes properties like minimal vapor pressure, good thermal and chemical durability, and a flexible character, recyclability, non-volatility, non-flammation, strong solubility capacity to a wide variety of substances, nonpolar and polar in nature [29,30].

Current aqueous amine approach has several significant limitations, ILs are particularly advantageous to be utilized as solvents for CO_2 absorption mainly because of the less energy required for solvent regeneration due to their physical absorption mechanism, where the van der Waals forces of attraction dominates the behavior of CO_2 dissolution in ILs [25]. However, chemical absorption is also observed in the case of some of the ILs such as the CO_2 + [bmim][Ac] system [31]. Several initiatives have been conducted by researchers in order to design - solvents that combine the excellent result of amines with the desired features of ionic liquids so that CO_2 can be absorbed selectively and efficiently from flue gases. Generally, this mixture of IL and amine is known as IL-amine hybrid solvent and the choice of IL can be from Room-temperature ionic liquids (RTILs) or Task-Specific Ionic Liquids (TSILs). Since amine-functionalized TSILs involves complex synthesis and purification processes, driving up manufacturing costs [24], therefore the more economical way is to use amine with commercially available RTILs only. The objective of this study to develop an ionic liquid amine hybrid solvent, and do all the required chemical and physically characterization for absorption of CO_2 at high pressure and furthermore the kinetic performance.

2. Materials and methods

2.1. Materials

Alkanolamines solvent of N- methyldiethanolamine (MDEA) with 98 % reagent grade ionic liquids (ILs) of 1-butyl-3-methylimidazolium dicyanamide [bmim][DCA] pureness of 98 %, 1-butyl-3-methylimidazolium acetate, [bmim][Ac] to the greatest reagent degree of 95 % and 1-butyl-3-methylimidazolium trifluoromethanesulfonate, [bmim][TfO] providing the reagent grade of 98 % were purchased from Merck Chemicals Sdn. Bhd. The ingredients were utilized without any further purification as it was regent grade chemicals. Gas Walkers Sdn. Bhd. in Malaysia supplied both the CO_2 and N_2 gases with 99.9 % purity.

2.2. Experimental approach for hybrid solvent preparation

Twelve (12) IL-amine hybrid solvents of different IL concentrations were prepared in this research work. In addition, a 30 wt% aqueous MDEA hybrid solvent was also prepared and to be used as a reference sample for comparison (Table 1). During sample preparation, 5 wt%, 10 wt%, 15 wt% and 20 wt% of [bmim][DCA], [bmim][Ac] and [bmim][TfO] were mixed with 30 wt% MDEA to form hybrid solvents. After sample preparation, prior to perform experiments, glass vials with tight-fitting screw lids were used to store all samples for at least 24 h at ambient temperature, which improved their total compatibility and prevented them from being contaminated with wetness.

2.3. Experimental investigation of thermo-physical properties of hybrid solvents

The density of aqueous hybrid solvents was measured using a digital Anton Par density meter (DMA-4500 M). To measure viscosity of aqueous hybrid solvents, the Anton Par Lovis-2000 M digital micro-viscometer equipped with an appropriate tube for capillary measurement. Refractive index of hybrid solvents was determined using digital Anton Paar Abbemat Refractometer while surface tension of aqueous hybrid solvents was determined using Tensiometer. Calibration was performed prior of all experiment using a standard water of Millipore quality for reliability, and the standard uncertainties u measurement values are put into consideration in terms of temperature and pressure values are u(T) = 0.01 K; u(P) = 0.01 bar, respectively.

Table 1
Comparison of experimental and literature data of CO_2 solubility of 30 wt% aqueous MDEA at 313.15 K.

Present work [a]		**Shen and Li** [32]		**Baek and Yoon** [33]	
P (bar)	α (mol/mol)	P (bar)	α (mol/mol)	P (bar)	α (mol/mol)
1.40	0.878	1.40	0.911	1.18	0.827
2.20	0.925	2.08	0.919	1.70	0.904
4.50	0.983	4.55	0.99	3.08	0.976
8.42	1.058	8.34	1.016	–	–
12.50	1.101	12.41	1.065	11.69	1.074
15.00	1.120	15.93	1.082	–	–

[a] Standard uncertainties u are u(T) = 0.01 K; u(P) = 0.01 bar and, Relative standard uncertainty $u_r(\alpha_{CO2}) = 0.106$.

2.4. Experimental approach for the investigation of CO_2 solubility

The pressure drop technique was used to determine the concentration of CO_2 in the hybrid solvents, in which the gas pressure in an equilibrium cell is tracked digitally as it fluctuates due to the solvent's uptake of CO_2. The pressure drop is caused by the bulk sorption of carbon dioxide into the hybrid solvents in a closed system [34,35]. Two equilibrium cells namely EC1 and EC2 are available and the capacity are 50 ml and 70 ml respectively. For both equilibrium cell EC1 and EC2, hybrid solvent samples occupied 10 % of the capacity, and the other ninety percent will be occupied by CO_2 gas vented from MV. After the apparatus is heated to desired temperature of 30 °C, pressurized CO_2 in the MV will be charge into the equilibrium cell and magnetic stirrer will be set at 300 rpm to enhance and maintain uniform solubility.

The experiment will be stopped when no further pressure drop was observed in equilibrium cell and equilibrium is achieved. From the measured results, there is a series of calculation need to be done for the evaluation of CO_2 solubility in the hybrid solvents as well as its kinetic study. Firstly, the number of moles of CO_2 will be determined from Equation (4) where the compressibility factors will be determined using the Peng Robison equation of state (EOS).

$$n_{CO_2} = \frac{V_T}{RT_a}\left[\frac{P_1}{Z_1} - \frac{P_2}{Z_2}\right] \tag{4}$$

where V_T is the volume of mixing vessel, R is the gas constant, T_a is the ambient temperature, P_1 is the pressure of mixing vessel before transfer CO_2, P_2 is the pressure of mixing vessel after transfer CO_2, Z_1 is the compressibility factor at P_1 and Z_2 is the compressibility factor at P_2.

Equilibrium pressure will be determined:

$$P_{C0_2} = P_T - P_V \tag{5}$$

where P_T is the total pressure of equilibrium cell and P_V is the vapor pressure of solvent in equilibrium cell.

The remaining moles of CO_2 in the EC (gas phase) is determined:

$$n_{g,CO_2} = \frac{V_g P_{CO_2}}{Z_{CO_2} RT} \tag{6}$$

where V_g is the volume of gas in equilibrium cell, P_{CO2} is the equilibrium pressure of CO_2, Z_{CO2} is the compressibility factor at P_{CO2}, R is the gas constant and T is the operating temperature.

The number of moles of CO_2 absorbed in solvent (liquid phase) will be calculated:

$$n_{l,CO_2} = n_{CO_2} - n_{g,CO_2} \tag{7}$$

Thus, the number of moles of the hybrid solvent is calculated:

$$n_{(ILs+Amine)} = \frac{\rho V_l m_{(ILs+Amine)_l}}{M_{(ILs+Amine)}} \tag{8}$$

where ρ is the density of solvent, V_l is the volume of solvent in equilibrium cell, $m_{(ILs+Amine)}$ is the mass fraction of ILs + Amine and $M_{(ILs+Amine)}$ is the molecular weight of ILs + Amine.

Since CO_2 solubility is defined as mole CO_2 per mole ILs-amine hybrid solvent, thus:

$$\alpha = \frac{n_{l,CO_2}}{n_{(ILs+Amine)}} \tag{9}$$

where α is the CO_2 loading capacity.

3. Results and discussion

3.1. Thermo-physical properties

Density of the prepared hybrid solvents were measured at the temperature range of 25–70 °C at the interlude of 5 °C while the pressure is kept constant at atmospheric pressure. The density date for aqueous MDEA-[bmim][DCA] hybrid solvent samples are tabulated in Table 2. Figs. 1-3 illustrates the density at 5 wt%, 10 wt%, 15 wt% and 20 wt% of [bmim][DCA], [bmim][Ac] and [bmim][TfO] respectively. The graphs of all hybrid solvents show the same trend as shown in Figs. 1, 2 and 3. However, of the three ILs under investigation, it was found out that hybrid solvents containing [bmim][TfO] exhibited the highest density as compared to hybrid solvents containing [bmim][Ac] and [bmim][DCA] as hybrid solvents at the same concentration of 5 wt%, 10 wt%, 15 wt% and 20 wt% ILs in the hybrid solvent. This finding makes sense given that the density of pure [bmim][TfO] is higher than pure [bmim][DCA] followed by pure [bmim][Ac].

Refractive index of the prepared hybrid solvents was examined in 5 degree increments between 25 and 70 °C. The refractive index for aqueous MDEA-[bmim][DCA] hybrid solvent sample is presented in Table 3. Figs. 4, 5 and 6 illustrates the refractive index at 5 wt%, 10 wt%, 15 wt% and 20 wt% of [bmim][DCA], [bmim][Ac] and [bmim][TfO] respectively. The refractive index determines how fast light can travel when entering the hybrid solvent [36].

By comparing the three ionic liquids under investigation, hybrid solvents containing [bmim][TfO] exhibited the lowest refractive index as compared to hybrid solvents containing [bmim][Ac] and [bmim][DCA] at the same concentration of 5 wt%, 10 wt%, 15 wt% and 20 wt% ILs. This might be due to at the same temperature, the molecules of [bmim][TfO] are loosely bonded with each other and moves faster, and thus the light to pass through faster and the refractive index is low [37].

Viscosity, defined as the resistance of a fluid to flow is one of the key determinants for the absorption of CO_2 especially during solvent regeneration. The viscosity data for aqueous MDEA-[bmim][DCA] hybrid solvent sample is given in Table 4. While the concentration of MDEA is maintained at 30 wt%, the viscosity of ionic liquid-amine hybrid solvent using [bmim][DCA], [bmim][Ac] and [bmim][TfO] with different mass ratios of 5 wt%, 10 wt%, 15 wt% and 20 wt% was noted at the range of 25–70 °C at the interlude of 5 °C as depicted in Fig. 7, Fig. 8 and Fig. 9 respectively. The higher the percentage of ionic liquid that is present in the hybrid solvent, the higher the viscosity of the solvent due to stronger intermolecular forces. The stronger the intermolecular forces, the tighter the molecules linked to each other, the higher the resistance of solvent to resist deformation and thus the viscosity increases. To add on, a minor increase in the percentage of the ionic liquid causes an equivalent increase in the resistance that exists internally between the molecules in the hybrid solvent as a result of the increased thickness of the ionic liquid related to the viscosity of MDEA naturally [38]. On the other hand, the viscosity of hybrid solvent decreases temperature because at higher temperature, a boost in molecular mobility and a reduction in molecular resistance to flow as a result of a change in either kinetic or thermal energy.

Table 2
The density data for aqueous MDEA-[bmim][DCA] hybrid solvent sample.

DENSITY TEMPERATURE	Sample			
	30 % MDEA + 5 % [bmim][DCA]	30 % MDEA + 10 % [bmim][DCA]	30 % MDEA + 15 % [bmim][DCA]	30 % MDEA + 20 % [bmim][DCA]
25	1.03000	1.03286	1.03511	1.03787
30	1.02744	1.03010	1.03219	1.03479
35	1.02476	1.02724	1.02919	1.03164
40	1.02197	1.02428	1.02610	1.02841
45	1.01906	1.02122	1.02293	1.02511
50	1.01604	1.01807	1.01966	1.02174
55	1.01289	1.01482	1.01633	1.01830
60	1.00967	1.01148	1.01290	1.01479
65	1.00634	1.00805	1.00940	1.01121
70	1.00291	1.00453	1.00581	1.00756

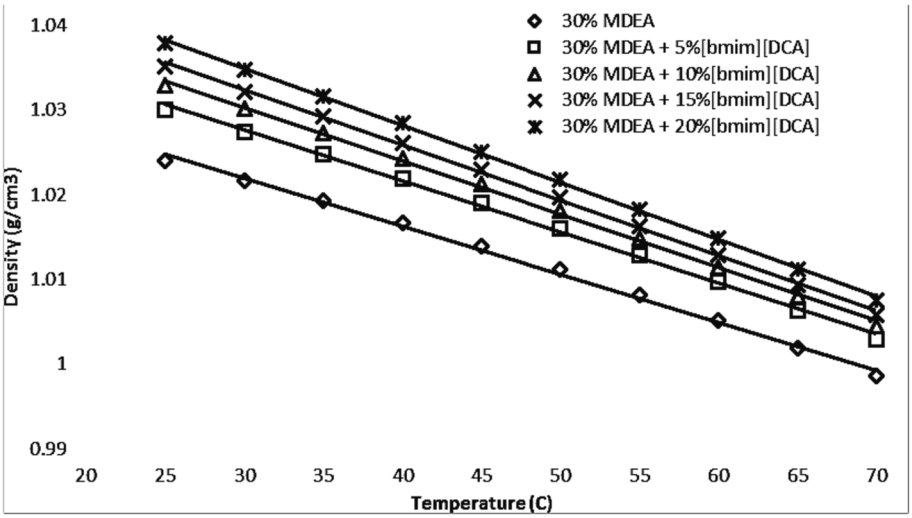

Fig. 1. Density for aqueous MDEA-[bmim][DCA] hybrid solvent sample.

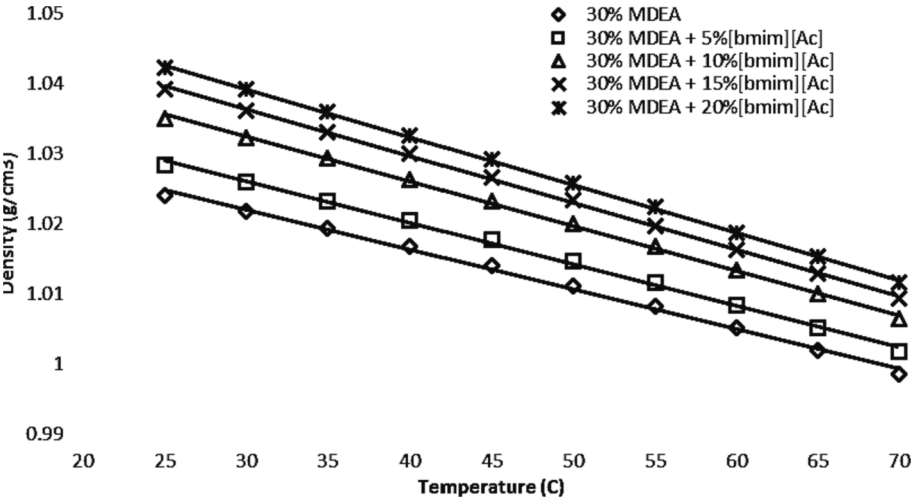

Fig. 2. Density for aqueous MDEA-[bmim][Ac] hybrid solvent sample.

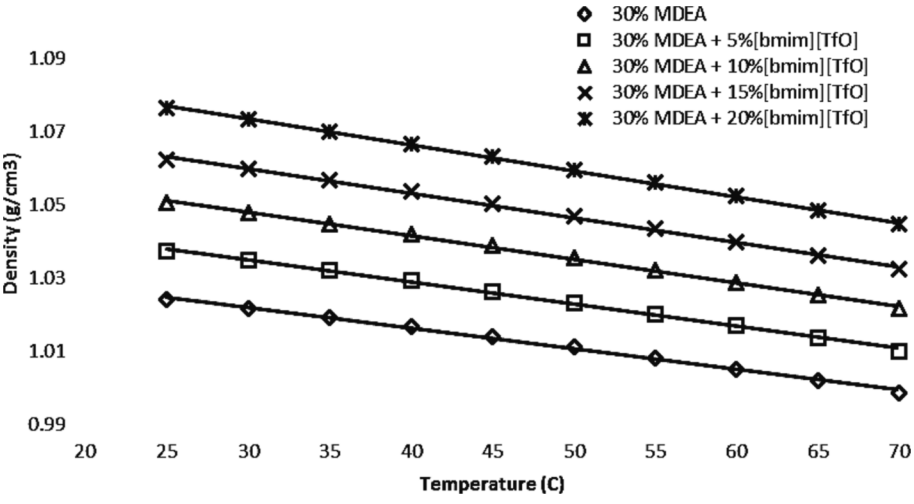

Fig. 3. Density for aqueous MDEA-[bmim][TfO] hybrid solvent sample.

Table 3
The refractive index data for aqueous MDEA-[bmim][DCA] hybrid solvent sample.

REFRACTIVE INDEX				
TEMPERATURE	Samples			
	30 % MDEA + 5 % [bmim][DCA]	30 % MDEA + 10 % [bmim][DCA]	30 % MDEA + 15 % [bmim][DCA]	30 % MDEA + 20 % [bmim][DCA]
25	1.384386	1.393078	1.401063	1.410289
30	1.383335	1.391978	1.399835	1.409030
35	1.382187	1.390710	1.398640	1.407741
40	1.381055	1.389538	1.397407	1.406427
45	1.379930	1.388304	1.396021	1.405069
50	1.378713	1.387024	1.394767	1.403654
55	1.377443	1.385716	1.393420	1.402345
60	1.376206	1.384411	1.392164	1.400925
65	1.374920	1.383131	1.390769	1.399485
70	1.373661	1.381932	1.389594	1.398239

From the results, it was found out that hybrid solvents with [bmim][TfO] IL has the lowest among the three hybrid solvents. It is known that the best hybrid solvent is the solvent with a lower viscosity because lower viscosity will help to increase the kinetics rate of absorption as well as to decrease the energy of solvent regeneration to save the energy cost [39]. Even though further investigation of other affecting parameters need to be conducted, from the viscosity point of view, hybrid solvent that comprises ILs [bmim][TfO] is a preferred solvent than [bmim][Ac] and [bmim][DCA].

The efficiency of solvents is highly depending on its surface tension. The surface layer of a liquid exhibits the properties of a flexible layer due to an effect known as surface tension. The surface tension of a liquid is due to the overall inside force felt by its molecules and the absorption efficiency of carbon dioxide could be enhanced by the induced surface tension in the system [40]. Surface tension of the prepared hybrid solvents were observed at the range of 25–70 °C over the span of 5 °C at atmospheric pressure. The surface tension data for aqueous MDEA-[bmim][DCA] hybrid solvent sample is illustrated in Table 5. Fig. 10, Fig. 11 and Fig. 12 illustrates the surface tension at 5 wt%, 10 wt%, 15 wt% and 20 wt% of [bmim][DCA], [bmim][Ac] and [bmim][TfO] respectively.

The results show that the surface tension of the solvent declines as the concentration of ionic liquid rises, mainly due to the ionic liquids that have inferior surface tension rate as equated to other constituents in the solvents such as water and MDEA at its pure form. Moreover, from the graphs, it is also observed that surface tension decreases with increasing temperature. The impact of increasing the temperature of

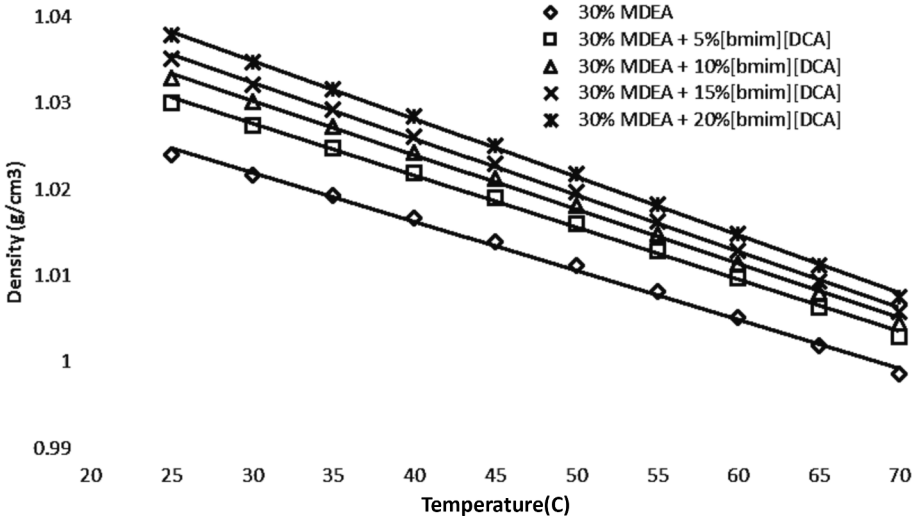

Fig. 4. The density for aqueous MDEA-[bmim][DCA] hybrid solvent sample.

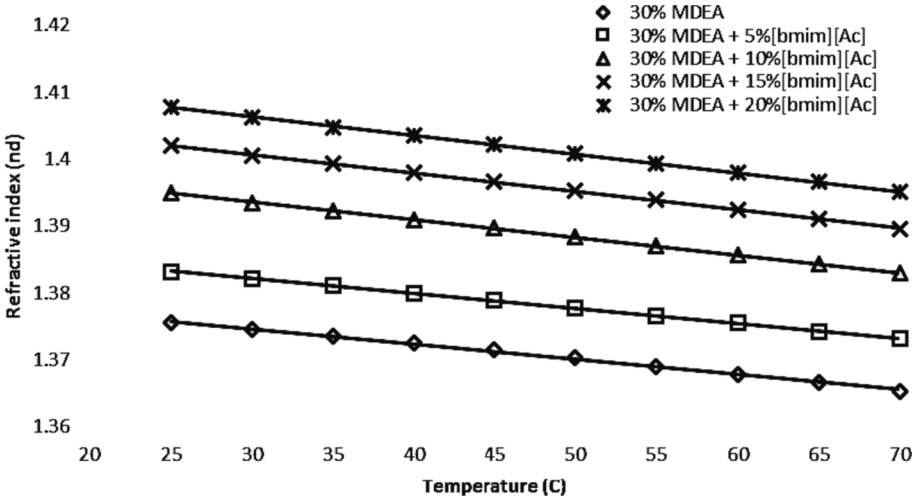

Fig. 5. Refractive index for aqueous MDEA-[bmim][Ac] hybrid solvent sample.

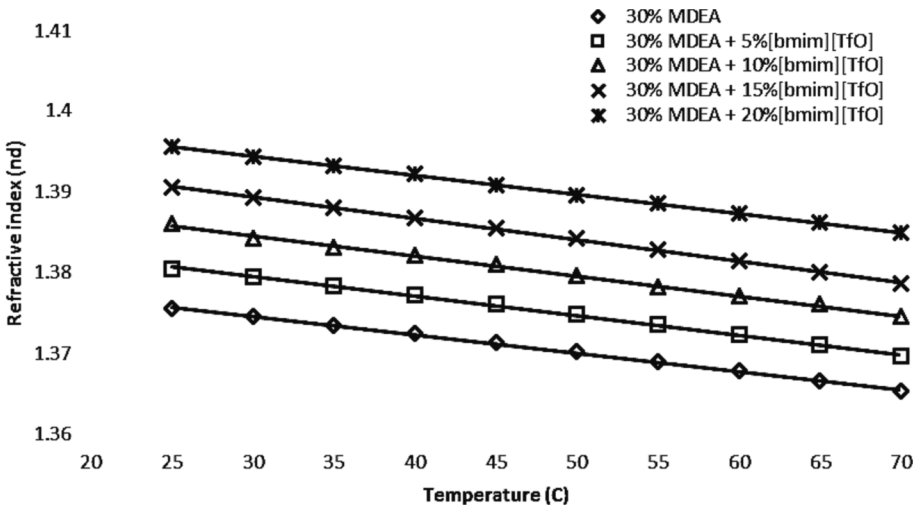

Fig. 6. Refractive index for aqueous MDEA-[bmim][TfO] hybrid solvent sample.

Table 4
The viscosity date for aqueous MDEA-[bmim][DCA] hybrid solvent sample.

VISCOSITY				
TEMPERATURE	Samples			
	30 % MDEA + 5 % [bmim] [DCA]	30 % MDEA + 10 % [bmim] [DCA]	30 % MDEA + 15 % [bmim] [DCA]	30 % MDEA + 20 % [bmim] [DCA]
25	3.4522	3.9874	4.5632	5.7251
30	2.9172	3.3041	3.8863	4.8657
35	2.4964	2.8226	3.3589	4.1931
40	2.1649	2.4426	2.9607	3.6145
45	1.9115	2.1502	2.6055	3.1802
50	1.6951	1.9261	2.4075	2.8340
55	1.5077	1.7667	2.2035	2.5335
60	1.3565	1.6707	2.0855	2.3853
65	1.2264	1.5626	2.0285	2.3083
70	1.1127	1.5332	1.9742	2.2894

solvent is to increase the molecular thermal energy, leading in a decline in cohesive forces and surface tension of the solvents. Pure ionic liquid [bmim][Ac] has highest surface tension values than pure [bmim][DCA] followed by pure [bmim][TfO] at a fix temperature and concentration. This is caused by the closer molecules of [bmim][Ac], resulting in a higher surface tension data for an aqueous mixture of MDEA with [bmim][Ac] as associated to the other two ILs at same temperature and composition.

3.2. CO_2 solubility in hybrid solvents

The CO_2 solubility of hybrid solvent at different concentrations of ILs were investigated by varying the pressure at 2 bar, 5 bar, 10 bar, 20 bar, 30 bar, 40 bar and 50 bar while maintaining the temperature at 30 °C. Similarly, to the thermo-physical properties, aqueous hybrid solvents were prepared by mixing 30 wt% MDEA with different ILs of 5 wt%, 10 wt%, 15 wt% and 20 wt%. The chosen ILs is the imidazolium based cation with long alkyl chain of 1-butyl-3-methylimidazolium [bmim] cation paired with different anions of [DCA], [Ac] and [TfO]. In addition, the CO_2 solubility of reference sample of aqueous 30 wt% of MDEA was tested to make comparison on the effect of adding ILs into conventional amine solvent. Figs. 13-15.

The effect of concentration of ILs was also investigated in this experiment. As exposed in Fig. 13, when the concentration of [bmim][DCA] rises to 5 wt% and 10 wt%, CO_2 solubility of hybrid solvent increases by approximately 48 % and 67 % at the same pressure of 10 bar. ILs increase the soluble nature of CO_2 in aqueous amine mixtures due to couplings with both the anion of the IL and CO_2 and the H proton of the C2 atom on the imidazole ring and CO_2 molecules [41]. However, when

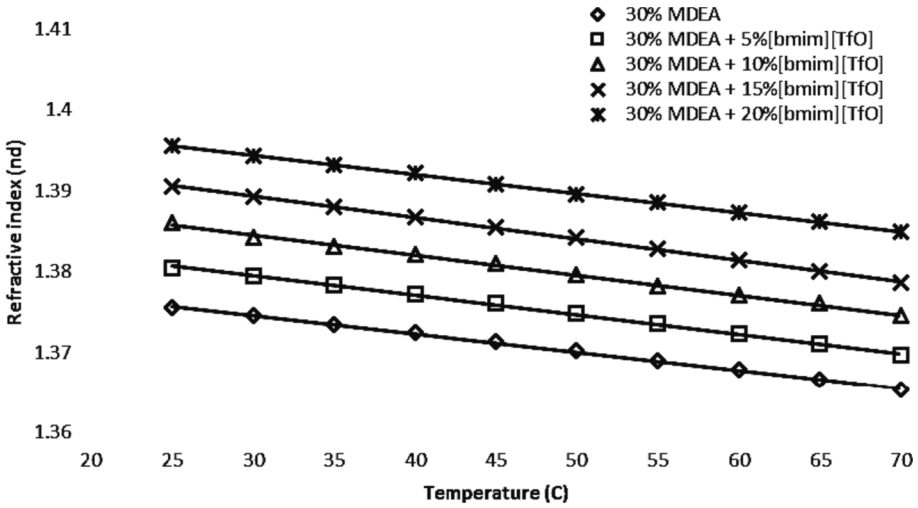

Fig. 7. Refractive index for aqueous MDEA-[bmim][DCA] hybrid solvent sample.

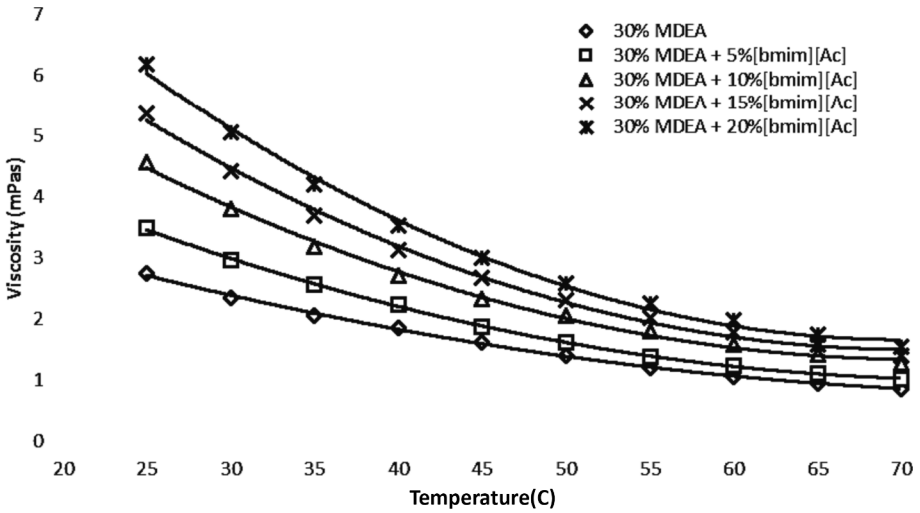

Fig. 8. Viscosity for aqueous MDEA-[bmim][Ac] hybrid solvent sample.

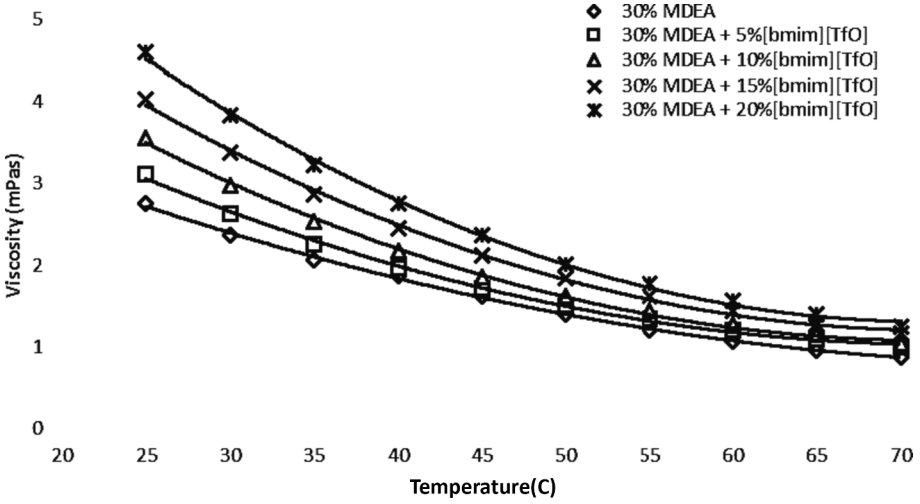

Fig. 9. Viscosity for aqueous MDEA-[bmim]TfO] hybrid solvent sample.

Table 5
The surface tension data for aqueous MDEA-[bmim][DCA] hybrid solvent sample.

SURFACE TENSION				
TEMPERATURE	Samples			
	30 % MDEA + 5 % [bmim][DCA]	30 % MDEA + 10 % [bmim][DCA]	30 % MDEA + 15 % [bmim][DCA]	30 % MDEA + 20 % [bmim][DCA]
25	54.360	52.128	50.402	47.760
30	53.620	51.584	49.710	47.030
35	53.096	51.034	49.068	46.324
40	52.520	50.508	48.420	45.746
45	52.078	49.960	47.744	45.216
50	51.656	49.436	47.100	44.856
55	50.948	48.820	46.798	44.452
60	50.416	48.428	46.556	44.268
65	49.832	47.942	46.222	43.916
70	49.216	47.368	45.738	43.550

the concentration of [bmim][DCA] is increased from 10 wt% to 15 wt%, the CO_2 solubility decreases and further decrease when the concentration of [bmim][DCA] reach 20 wt%. The reason behind this decrement in CO_2 solubility is mainly due to the high concentration of [bmim][DCA] results in a highly viscous solvent which has higher resistance to motion leading to lower absorption capacity. Moreover, at high concentration of IL, the non-uniform interfacial distribution on the surface results in a lower surface tension which speeds up the CO_2 absorption rate. As presented in Fig. 14 and Fig. 15, similar trend is observed for hybrid solvents containing [bmim][Ac] and [bmim][TfO]. By making comparison at 10 bar, when the concentration of [bmim][Ac] increased to 5 wt% and 10 wt%, the CO_2 loading increased by 35 % and 32 % respectively while when the concentration of [bmim][Ac] increased to 15 wt% and 20 wt% the CO_2 loading is reduced by 12 % and 27 %. Similarly, an increment in CO_2 loading is observed for hybrid solvents containing [bmim][TfO] when the concentration is increased up to 10 wt%. Beyond 10 wt%, the CO_2 loading decreased because of the hybrid solvent's excessive viscosity.

As illustrated in Fig. 13, Fig. 14 and Fig. 15, as the pressure increases from 2 bar to 50 bar, the CO_2 solubility of all hybrid solvents increases. This is because at higher pressure, more CO_2 can dissolve and diffuse into the hybrid solvent to relieve the high pressure in a closed vessel of equilibrium cell. Most importantly, when the results is compared with the reference sample of aqueous 30 wt% MDEA, all hybrid solvents showed a steeper gradient, meaning to say the addition of small amount of ILs into conventional amine solution has a significant effect in

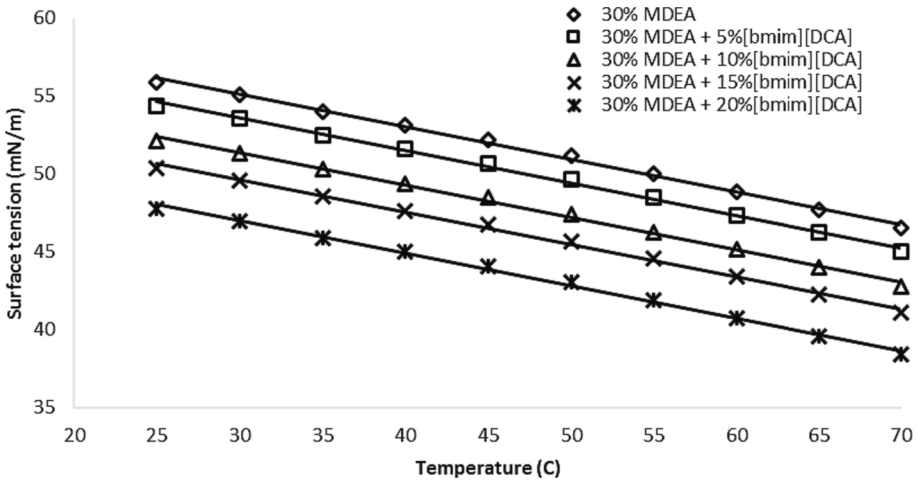

Fig. 10. Surface tension for aqueous MDEA-[bmim][DCA] hybrid solvent sample.

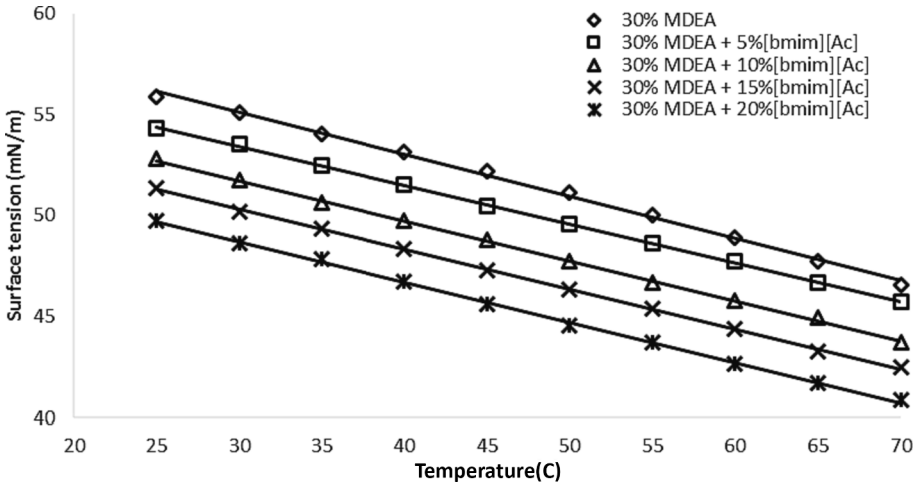

Fig. 11. Surface tension for aqueous MDEA-[bmim][Ac] hybrid solvent sample.

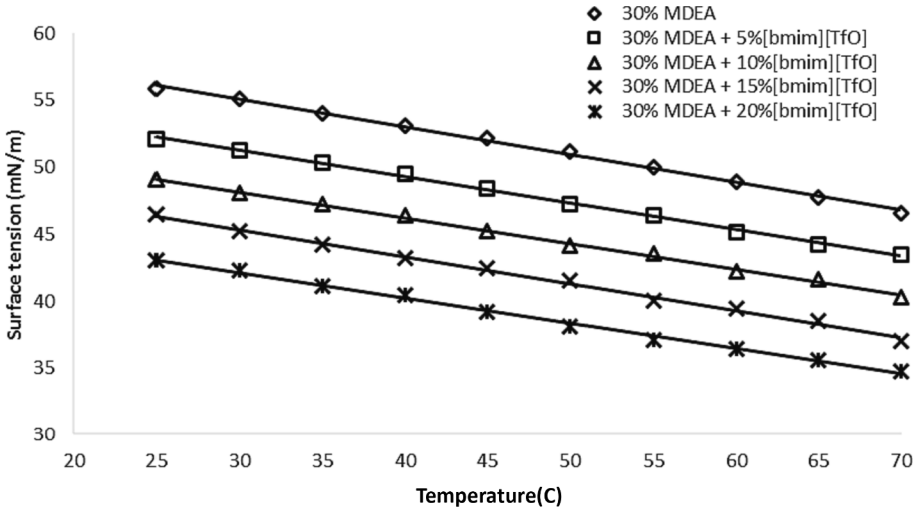

Fig. 12. Surface tension for aqueous MDEA-[bmim][TfO] hybrid solvent sample.

boosting the dissolution of CO_2 in synthetic solvents.

The goal is to identify the most effective hybrid solvent for absorbing CO_2, the results of hybrid solvent with the highest CO_2 loading from each ILs are extracted and plotted in Fig. 16. Obviously, the hybrid solvent containing 10 wt% [bmim][TfO] has the highest CO_2 loading and thus it has the best CO_2 absorption performance among all hybrid

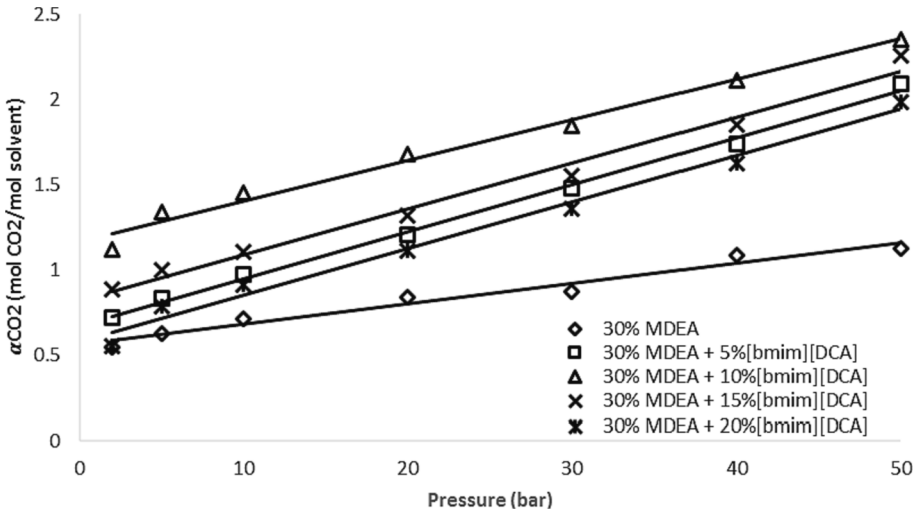

Fig. 13. CO_2 loading for aqueous MDEA-[bmim][DCA] hybrid solvent sample.

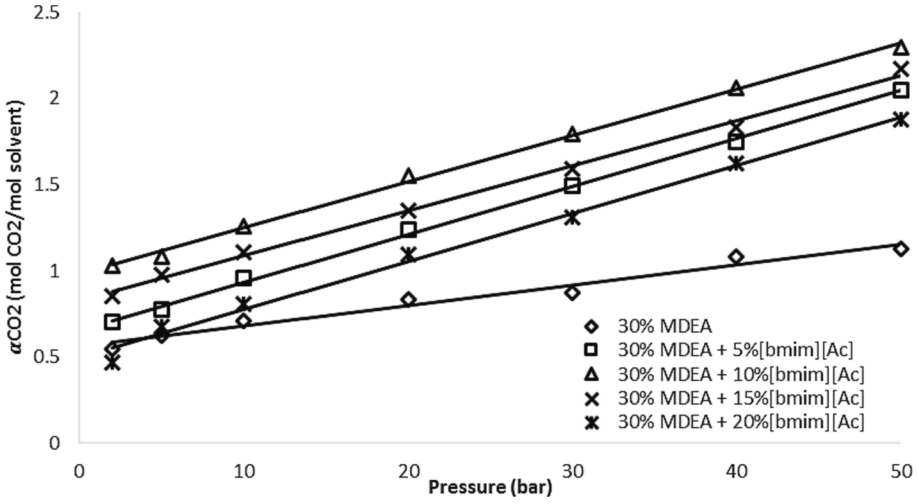

Fig. 14. CO_2 loading for aqueous MDEA-[bmim][Ac] hybrid solvent sample.

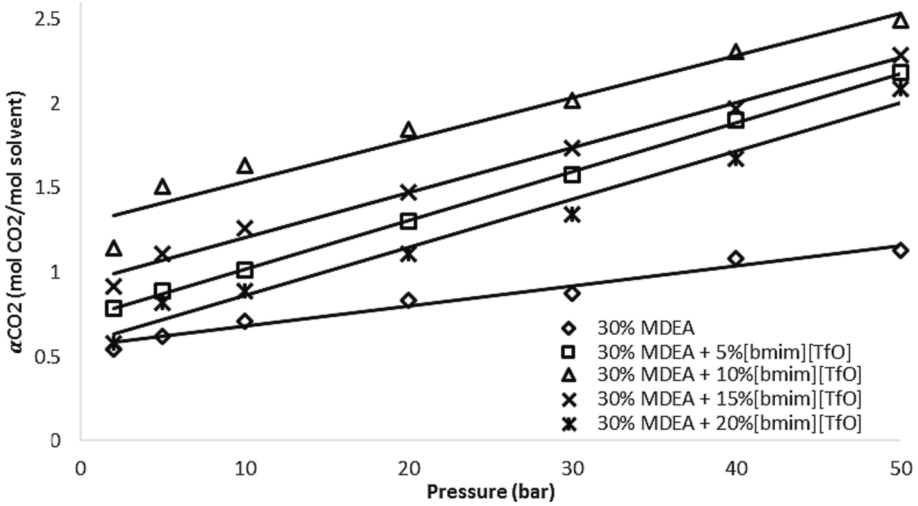

Fig. 15. CO_2 loading for aqueous MDEA-[bmim][TfO] hybrid solvent sample.

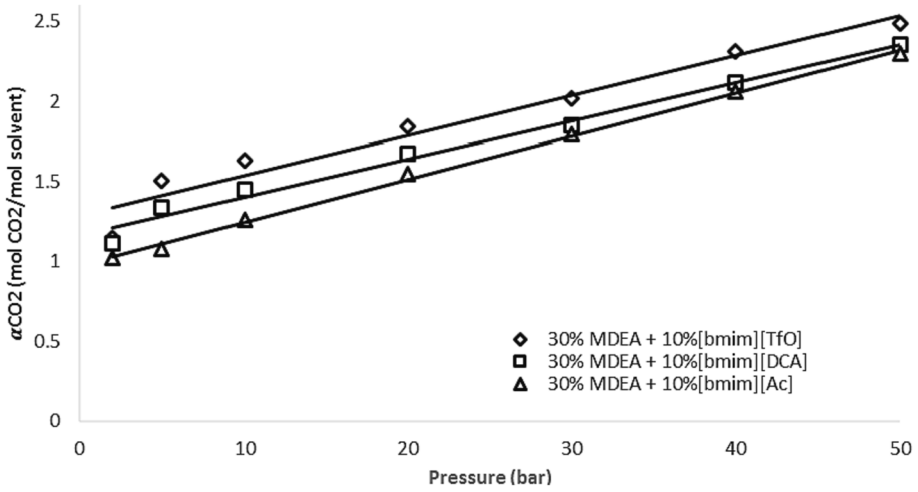

Fig. 16. Hybrid solvent with the highest CO_2 loading from each ILs.

solvents. This is mainly because of higher CO_2 solubility in fluorine-modified IL compared to natural IL such as [bmim][DCA] and [bmim][Ac] due to the greater free volume of [bmim][TfO] and fluorinated alkyl groups interact with carbon dioxide more strongly. Furthermore, this result is expected because from the thermo-physical properties investigation, the hybrid solvent containing [bmim][TfO] shows the lowest viscosity as compared with the other two ILs. Hybrid solvent with low viscosity is identified to have a higher absorption rate and lower regeneration energy as the solvent will have weaker intermolecular forces [42]. In addition, the hybrid solvent containing [bmim][TfO] shows the lowest surface tension as compared with the other two ILs which is then believed to help increase the efficiency of absorbing the CO_2.

3.3. Absorption kinetics in hybrid solvents

The absorption kinetics of aqueous hybrid solvents can be analyzed from the CO_2 solubility data with the time interval of 30 min at constant pressure and temperature. In this study, CO_2 solubility data for hybrid solvents of 30 wt% MDEA mixed with [bmim][DCA], [bmim][Ac] and [bmim][TfO] of 5 wt%, 10 wt%, 15 wt% and 20 wt% at 5 bar and 30 °C were analyzed. The ability to dissolve carbon dioxide in hybrid solvents is reflected in their CO_2 capacity for absorption. As shown in Fig. 17, Fig. 18 and Fig. 19, the CO_2 absorption rate increases when the concentration of ILs increases from 0 wt% to 5 wt% and 10 wt%. This prove that the addition of ILs helps to boost the CO_2 absorption rate. However, the CO_2 absorption rate drops at IL concentrations of 15 wt% and 20 wt %. A highly viscous solvent will lead to low CO_2 absorption capacity and high regeneration energy due to a higher resistance to motion changes [43]. Furthermore, low surface tension will lead to slow CO_2 absorption rate. Since similar trends were observed from all hybrid solvents containing [bmim][DCA], [bmim][Ac] and [bmim][TfO], therefore it can be concluded that the optimum ILs concentration to be used for process optimization is 10 wt% before the reverse effect takes place due to high viscosity and low surface tension. This is because by optimizing the amount of ILs to be used, the operating cost of the process can be reduced.

The results of hybrid solvent with the highest CO_2 absorption rate from each ILs are extracted and plotted in Fig. 20. By comparison, the hybrid solvent containing 10 wt% [bmim][TfO] has the highest CO_2 absorption rate, meaning that the hybrid solvent can absorb more CO_2 at a shorter time. This is because [TfO]-anion-containing IL has a far greater attraction to CO_2 than [DCA]- and [Ac]-anion-containing IL. This result is expected as portrayed in the thermo-physical properties investigation and CO_2 solubility test. The results were dominated by the viscosity effect while the surface tension, refractive index and density of hybrid solvents were seemed to have less influence to CO_2 absorption kinetics.

Since aqueous MDEA-10 wt% [bmim][TfO] hybrid solvent has the uppermost CO_2 uptake and highest CO_2 absorption rate, the CO_2

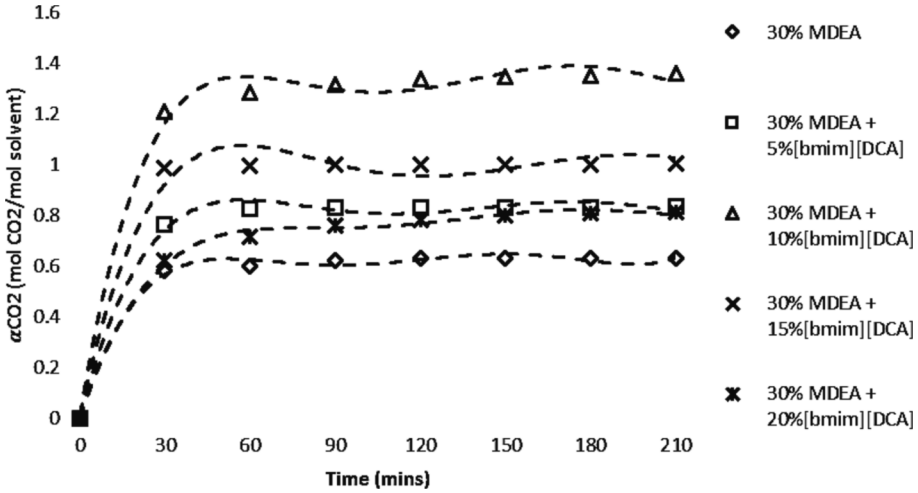

Fig. 17. CO_2 absorption rate of aqueous MDEA-[bmim][DCA] hybrid solvents at 5 bar.

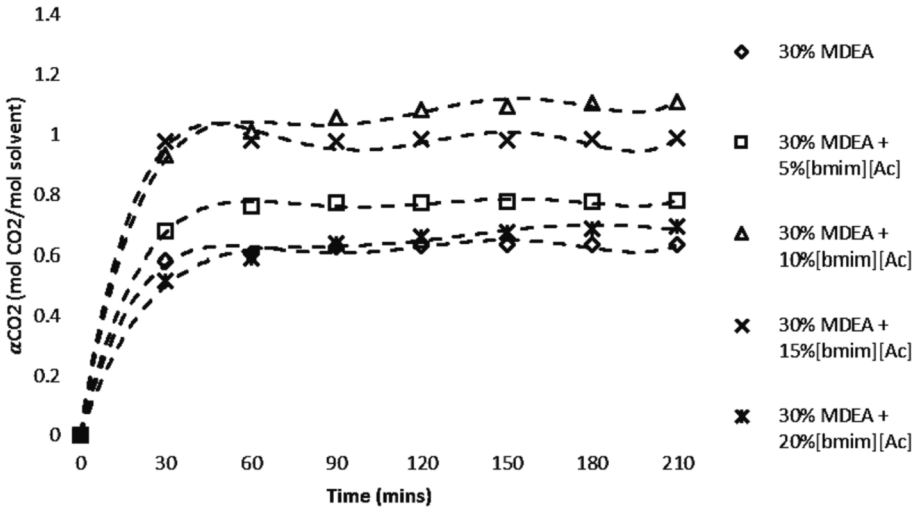

Fig. 18. CO_2 absorption rate of aqueous MDEA-[bmim][Ac] hybrid solvents at 5 bar.

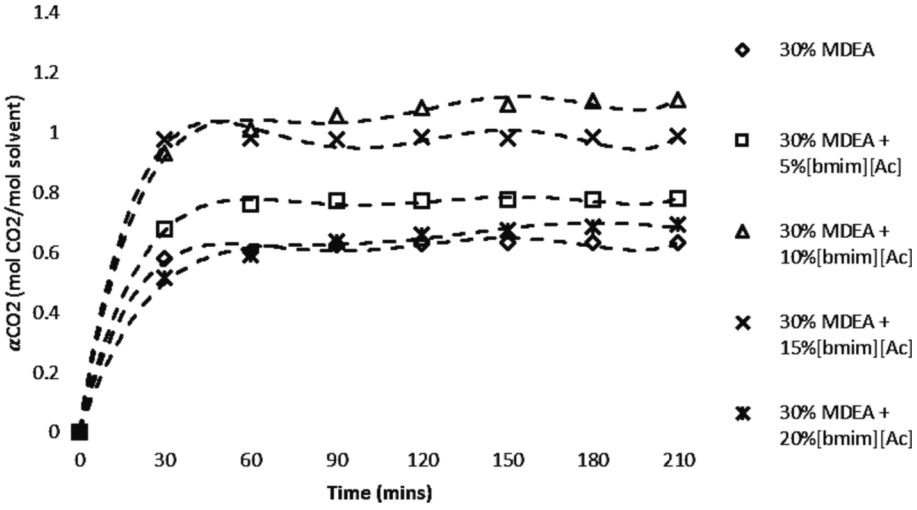

Fig. 19. CO_2 absorption rate of aqueous MDEA-[bmim][TfO] hybrid solvents at 5 bar.

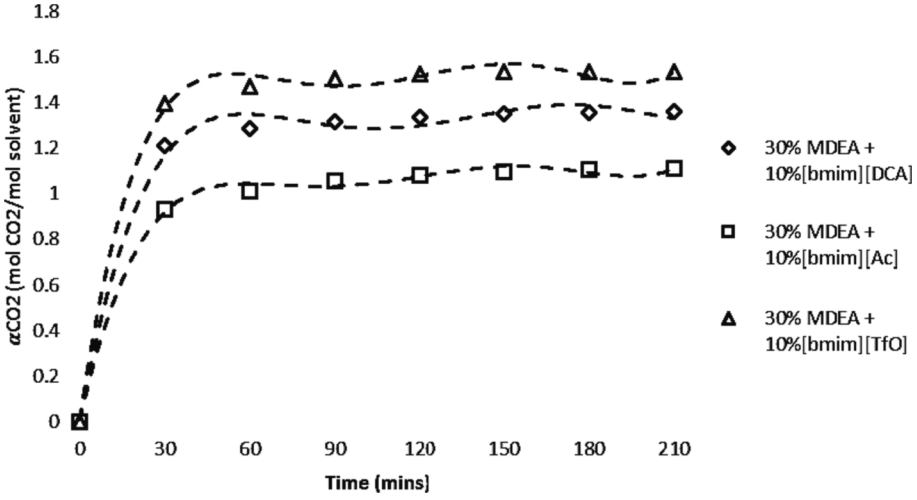

Fig. 20. Hybrid solvent with the highest CO_2 absorption rate from each ILs at 5 bar.

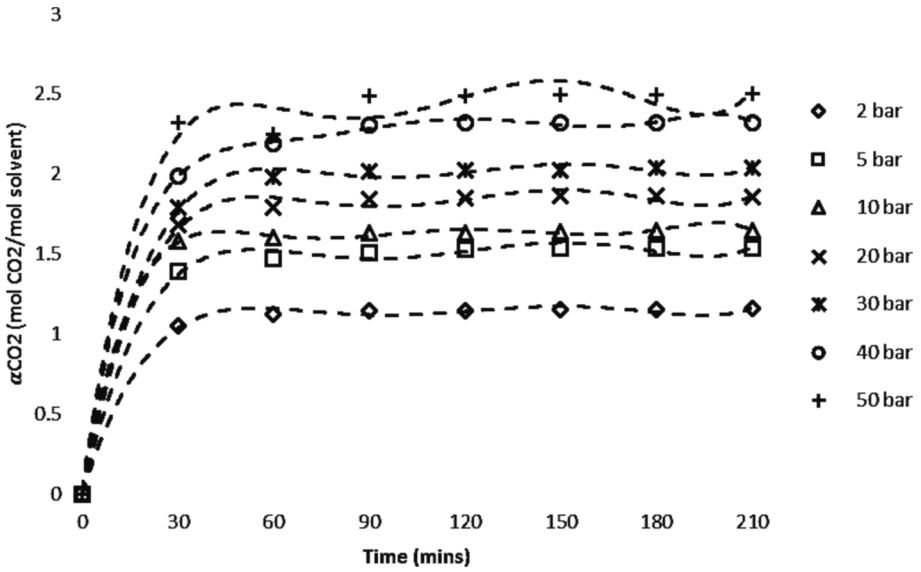

Fig. 21. CO_2 absorption rate of aqueous MDEA-10 wt% [bmim][TfO] hybrid solvent at different pressure.

absorption kinetics of the synthetic solvent at temperature change of 2 bar to 50 bar was further analyzed. As given in Fig. 21, it is noted that when the pressure surges from 2 to 50 bar, the CO_2 loading rises, and the highest CO_2 loading is at 50 bar. This is because more CO_2 can diffuse into the hybrid solvent until the partial pressures across the CO_2-solvent interface are equilibrated. On the other hand, by observing at the gradient of the graph at the first 30 min, 50 bar of pressure has the highest CO_2 absorption kinetics. This can be explained by the trend illustrated in the Fig. 21 whereby the steeper the gradient of the graph, the higher the CO_2 absorption kinetics as more CO_2 number of moles can be absorbed per mole of hybrid solvents within 30 min. The CO_2 loading of the hybrid solvent start to stabilize after 60 min until equilibrium is achieved.

4. Conclusion

This is a new investigation, presented here on the thermo-physical properties of the ILs-amine hybrid solvents with the aim of investigating the CO_2 loading capacity and absorption rate. 30 wt% (MDEA) was blended with three imidazolium-based ILs: [bmim][DCA], [bmim][Ac] and [bmim][TfO] at concentrations of 5 wt%, 10 %, 15 wt% and 20 wt%. The investigation of thermo-physical properties of prepared hybrid solvents at the range of 25-70°Cover the span of 5 °C using 5 wt %, 10 wt%, 15 wt% and 20 wt% of [bmim][DCA], [bmim][Ac] and [bmim][TfO] demonstrated thermo-physical characteristics including density, refractive index, viscosity, and surface tension decrease with increasing temperature. However, beyond 60 °C, the effect of temperature on viscosity is insignificant. On the other hand, when the amount of ILs rises, the density, refractive index and viscosity increases while the surface tension decreases. Then, CO_2 loading capacity in hybrid solvents was determined using pressure decay approach, at different pressure range from 2 bar to 50 bar. It was observed that the hybrid solvent having 10 wt% [bmim][TfO] has the uppermost CO_2 loading among all hybrid solvents. Furthermore, it was determined that the optimum concentration of IL is 10 wt% for process optimization. It is recommended that the concentration of the IL to be not more than 10 wt%. Beyond 10 wt% of ILs, the CO_2 solubility decreases due to high viscosity. To add on, [bmim][TfO] is fluorine-substituted IL and therefore it has a higher CO_2 affinity than normal IL such as [bmim][DCA] and [bmim][Ac]. From the analysis of CO_2 solubility data, hybrid solvent containing 10 wt% [bmim][TfO] has the highest CO_2 absorption kinetics, thus it can absorb more CO_2 at a shorter time as compared to other hybrid solvents. This result is expected as portrayed in the thermo-physical properties investigation and CO_2 solubility test. Looking at the pressure effect on CO_2 absorption kinetics of aqueous MDEA-10 wt% [bmim][TfO] hybrid solvent, it was found out that at higher pressure, more CO_2 can dissolve in the hybrid solvent at a given time to relieve the pressure in a closed vessel. The highest CO_2 absorption kinetics is recorded at 50 bar. In a nutshell, ILs-amine hybrid solvent is proven to enhance CO_2 absorption performance. All the results are dominated by the viscosity effect while the surface tension, refractive index and density of hybrid solvents were seemed to have less influence to CO_2 absorption performance. Furthermore, it is also found out that fluorinated anion in ILs has a higher CO_2 affinity than the non-fluorinated anions. ILs-amine hybrid solvents are proven to be a promising solvent for CO_2 capture in the future. More combinations of hybrid solvents from different cations and anions are recommended for further investigation in the future work.

CRediT authorship contribution statement

Saleem Nawaz Khan: . **Faheem Abbas:** Methodology, Software. **Francis M. Enujekwu:** Supervision, Project administration. **Sami Ullah:** Funding acquisition. **Mohammed Ali Assiri:** Methodology, Investigation. **Abdullah G. Al-Sehemi:** Formal analysis.

Declaration of Competing Interest

The authors declare that they have no known competing financial interests or personal relationships that could have appeared to influence the work reported in this paper.

Data availability

Data will be made available on request.

Acknowledgement

The authors extend their appreciation to the Ministry of Education in KSA for funding this research work through the project number KKU-IFP2-DA-10.

References

[1] Administration, U.S.E.I., International Energy Outlook 2016. 2016, U.S. Department of Energy: Washington, DC. p. 276.

[2] M. Abunowara, et al., Characterization of mukah-balingian and merit-pila coals before and after subcritical CO_2 exposure using surface-area techniques, J. Environ. Eng. 146 (8) (2020) 04020087.
[3] A. Kavoosi, Consequences of global demand and supply of fossil energy and the need to use wind energy as a potential in Iran, Anthropogenic Pollution 5 (1) (2021) 98–104.
[4] S. Das, T. Ben, A [COF-300]-[UiO-66] composite membrane with remarkably high permeability and H2/CO2 separation selectivity, Dalton Trans. 47 (21) (2018) 7206–7212.
[5] T.E. Rufford, et al., The removal of CO_2 and N_2 from natural gas: A review of conventional and emerging process technologies, J. Pet. Sci. Eng. 94–95 (2012) 123–154.
[6] D. Dortmundt, K. Doshi, Recent developments in CO_2 removal membrane technology. UOP LLC, 1999.
[7] S. Ullah, et al., Synthesis, CO_2 adsorption performance of modified MIL-101 with multi-wall carbon nanotubes, Adv. Mat. Res. 1133 (2016) 486–490.
[8] S. Ullah, et al., The role of multiwall carbon nanotubes in Cu-BTC metal-organic frameworks for CO_2 adsorption, J. Chin. Chem. Soc. 63 (12) (2016) 1022–1032.
[9] M. Kanniche, et al., Pre-combustion, post-combustion and oxy-combustion in thermal power plant for CO_2 capture, Appl. Therm. Eng. 30 (1) (2010) 53–62.
[10] F.A. Abdul Kareem, et al., Experimental measurements and modeling of supercritical CO_2 adsorption on 13X and 5A zeolites, J. Nat. Gas Sci. Eng. 50 (2018) 115–127.
[11] M. Abunowara, et al., Experimental and theoretical investigations on kinetic mechanisms of low-pressure CO_2 adsorption onto Malaysian coals, J. Nat. Gas Sci. Eng. 88 (2021), 103828.
[12] F.A. Abdul Kareem, et al., Adsorption of pure and predicted binary (CO2:CH4) mixtures on 13X-Zeolite: Equilibrium and kinetic properties at offshore conditions, Microporous Mesoporous Mater. 267 (2018) 221–234.
[13] D.Y.C. Leung, G. Caramanna, M.M. Maroto-Valer, An overview of current status of carbon dioxide capture and storage technologies, Renew. Sustain. Energy Rev. 39 (2014) 426–443.
[14] E. Torralba-Calleja, J. Skinner, D. Gutierrez-Tauste, CO_2 capture in ionic liquids: a review of solubilities and experimental methods, J. Chem. (2013).
[15] M. Babar, et al., Sustainable functionalized metal-organic framework NH2-MIL-101 (Al) for CO2 separation under cryogenic conditions, Environ. Pollut. 279 (2021), 116924.
[16] M. Babar, et al., Enhanced cryogenic packed bed with optimal CO_2 removal from natural gas; a joint computational and experimental approach, Cryogenics 105 (2020), 103010.
[17] S. Saqib, et al., Influence of interfacial layer parameters on gas transport properties through modeling approach in MWCNTs based mixed matrix composite membranes, Chem. Eng. Sci. (2020), 115543.
[18] S. Ullah, et al., High-temperature CO_2 removal from CH_4 using silica membrane: experimental and neural network modeling, Greenhouse Gases Sci. Technol. 9 (5) (2019) 1010–1026.
[19] S. Ullah, et al., Synthesis, and characterization of metal-organic frameworks -177 for static and dynamic adsorption behavior of CO_2 and CH_4, Microporous Mesoporous Mater. 288 (2019), 109569.
[20] S. Ullah, et al., Synthesis and characterization of mesoporous MOF UMCM-1 for CO_2/CH_4 adsorption; an experimental, isotherm modeling and thermodynamic study, Microporous Mesoporous Mater. 294 (2020), 109844.
[21] S. Ullah, et al., Synthesis and characterization of iso-reticular metal-organic Framework-3 (IRMOF-3) for CO2/CH4 adsorption: Impact of post-synthetic aminomethyl propanol (AMP) functionalization, J. Nat. Gas Sci. Eng. 72 (2019), 103014.
[22] S. Ullah, et al., CO_2 solubility and thermophysical properties in aqueous mixtures of piperazine and diethanolamine, Sustainable Energy Technol. Assess. 53 (2022), 102514.
[23] S. Babamohammadi, A. Shamiri, M.K. Aroua, A review of CO_2 capture by absorption in ionic liquid-based solvents, Rev. Chem. Eng. 31 (4) (2015) 383–412.
[24] E.I. Privalova, et al., Capturing CO_2: conventional versus ionic-liquid based technologies, Russ. Chem. Rev. 81 (5) (2012) 435–457.
[25] M. Ramdin, T.W. de Loos, T.J.H. Vlugt, State-of-the-Art of CO_2 Capture with Ionic Liquids, Ind. Eng. Chem. Res. 51 (24) (2012) 8149–8177.
[26] J. Yang, et al., CO_2 capture using amine solution mixed with ionic liquid, Ind. Eng. Chem. Res. 53 (7) (2014) 2790–2799.
[27] L.Y. Zhou, et al., Solubilities of CO_2, H_2, N_2 and O_2 in ionic liquid 1-n-butyl-3-methylimidazolium heptafluorobutyrate, J. Chem. Thermodyn. 59 (2013) 28–34.
[28] J.H. Huang, T. Ruther, Why are ionic liquids attractive for CO_2 absorption? An overview, Australian J. Chem. 62 (4) (2009) 298–308.
[29] S. Ullah, et al., Experimental investigation and modeling of the density, refractive index, and dynamic viscosity of 1-Propyronitrile-3-Butylimidazolium Dicyanamide, J. Mol. Liq. 302 (2020), 112470.
[30] G. Gonfa, et al., Density and excess molar volume of binary mixture of thiocyanate-based ionic liquids and methanol at temperatures 293.15–323.15 K, J. Mol. Liq. 211 (2015) 734–741.
[31] A. Yokozeki, et al., Physical and chemical absorptions of carbon dioxide in room-temperature ionic liquids, J. Phys. Chem. B 112 (51) (2008) 16654–16663.
[32] K.P. Shen, M.H. Li, Solubility of carbon dioxide in aqueous mixtures of monoethanolamine with methyldiethanolamine, J. Chem. Eng. Data 37 (1) (1992) 96–100.
[33] J.-I. Baek, J.-H. Yoon, Solubility of carbon dioxide in aqueous solutions of 2-amino-2-methyl-1, 3-propanediol, J. Chem. Eng. Data 43 (4) (1998) 635–637.
[34] S. Ullah, et al., Reactive kinetics of carbon dioxide loaded aqueous blend of 2-amino-2-ethyl-1,3-propanediol and piperazine using a pressure drop method, Int. J. Chem. Kinet. 51 (4) (2019) 291–298.
[35] S.N. Khan, et al., Thermophysical properties of concentrated aqueous solution of N-methyldiethanolamine (MDEA), piperazine (PZ), and ionic liquids hybrid solvent for CO2 capture, J. Mol. Liq. 229 (2017) 221–229.
[36] K. Biernacki, et al., Physicochemical properties of choline chloride-based deep eutectic solvents with polyols: an experimental and theoretical investigation, ACS Sustain. Chem. Eng. 8 (50) (2020) 18712–18728.
[37] R. Phadagi, et al., Understanding the role of Dimethylformamide as co-solvents in the dissolution of cellulose in ionic liquids: Experimental and theoretical approach, J. Mol. Liq. 328 (2021), 115392.
[38] S.N. Khan, et al., Thermophysical properties of aqueous 1-butyl-3-methylimidazolium acetate [BMIM][AC]+ monoethanolamine (MEA) hybrid as a solvent for CO2 capture, Procedia Eng. 148 (2016) 1326–1331.
[39] F.O. Ochedi, et al., Carbon dioxide capture using liquid absorption methods: a review, Environ. Chem. Lett. 19 (2021) 77–109.
[40] P. Muchan, et al., Amine structure-foam behavior relationship and its predictive foam model used for amine selection for design of amine-based carbon dioxide (2) capture process, Curr. Chin. Sci. 1 (1) (2021) 43–57.
[41] Y. Qu, et al., Amino acid ionic liquids as efficient catalysts for CO_2 capture and chemical conversion with epoxides under metal/halogen/cocatalyst/solvent-free conditions, Sustainable Energy Fuels 5 (9) (2021) 2494–2503.
[42] D. Malhotra, et al., Directed hydrogen bond placement: low viscosity amine solvents for CO_2 capture, ACS Sustain. Chem. Eng. 7 (8) (2019) 7535–7542.
[43] S. Tiwari, et al., A strategy of development and selection of absorbent for efficient CO_2 capture: An overview of properties and performance, Process Saf. Environ. Prot. 163 (2022) 244–273.